High-rate deposition of $YBa_2Cu_3O_{7-x}$ films by hot cluster epitaxy

Yuzuru Takamura,[a] Norio Yamaguchi,[b] Kazuo Terashima, and Toyonobu Yoshida
Department of Metallurgy and Materials Science, Graduate School of Engineering, The University of Tokyo, Hongo 7-3-1, Bunkyo-ku, Tokyo 113-8656, Japan

(Received 29 June 1998; accepted for publication 23 July 1998)

The growth rate and crystallinity of $YBa_2Cu_3O_{7-x}$ (YBCO) films were investigated in connection with the cluster size and the growth mode in order to clarify the high-rate deposition of high-quality epitaxial films from clusters in the plasma flash evaporation method. The films were deposited from clusters that were not accelerated by bias voltage but were self-activated in a thermal plasma. With increasing cluster size, the growth rate increased drastically at the point of the growth mode transition from spiral to two-dimensional cluster nucleus growth. After the transition, the film was still well epitaxial and have the minimum value of the full width at half maximum of the (005) x-ray rocking curve ($FWHM_{rc}$). A 1-μm-thick, nonspiral growth, monolayer smooth epitaxial YBCO film was successfully deposited at a growth rate of 16 nm/s. $FWHM_{rc}$ for the films was less than 0.14°. It was revealed experimentally that the deposition from "hot" clusters with large sticking probability onto a high-temperature substrate is highly effective for the deposition of high-quality films at a high rate. © *1998 American Institute of Physics.* [S0021-8979(98)01721-6]

I. INTRODUCTION

Multicomponent materials such as high critical temperature (T_c) superconductors (HTSCs) have become more interesting and attractive in both scientific and engineering fields. From the viewpoint of materials processing, the development of a high-rate epitaxial film deposition method is expected.

Thermal plasma processing methods such as spraying and thermal plasma chemical vapor deposition are promising candidates for high-rate deposition, because of the high density of reactive particles.[1] Among them, the plasma flash evaporation (PFE) method[2] has some interesting characteristics such as high-rate and large-area deposition of multicomponent systems under various reactive soft-vacuum (about 200 Torr) atmospheres (Fig. 1). In this method, mixed fine powders of constituents are continuously injected into a rf plasma so that they are evaporated completely and codeposited on a substrate. This method has been applied to HTSC film preparation, and epitaxial $YBa_2Cu_3O_{7-x}$ (YBCO) films with excellent properties ($T_c = 92$ K, $J_c = 8\times10^5$ A/cm^2) have been successfully deposited in a relatively large area of 7 cm×7 cm.[3–6]

Recently, the prominent feature of this process was revealed to be the deposition from clusters under high atomic oxygen flux generated in a plasma flame.[6] In PFE, nanometer-scale clusters are formed under the high supersaturation of evaporated materials quenched from 5000 to 1000 K in the boundary layer. The clusters are considered not to be accelerated by bias voltage but self-activated into the "hot" and unstable state and to have some size distribution in thermal plasma. Our previous study revealed that the epitaxial growth modes existing in YBCO film deposition from clusters are divided into two mechanisms as shown in Fig. 2 according to the clusters' average size,[7] which was estimated by the microtrench method.[8] When most of the incoming three-dimensional (3D) clusters are smaller than the two-dimensional (2D) critical nucleus size (r^*_{2D}), the clusters may evaporate onto a surface and films grow spirally similar to the growth from atoms. On the other hand, when the powder feed rate is increased and some 3D clusters are larger than r^*_{2D}, the clusters supply stable 2D nuclei and serve as steps of epitaxial growth sites, arround which atoms from clusters smaller than r^*_{2D} grow. In this case, films can grow without help of screw dislocations like 2D nucleus growth (2DNG). Here, we call this incoming-cluster stimulated 2D nucleus growth "2D cluster nucleus growth (2DCNG)," because 2D nuclei are formed directly from incoming clusters. In these modes, large clusters are considered to rearrange into an epitaxial crystal structure due to thermal energy, with the help of the internal energy of clusters. Therefore, we name this process "hot cluster epitaxy (HCE)." HCE is expected to have a high possibility of depositing an excellent film at an extremely high growth rate. However, systematic studies of the growth rate and the crystallinity of film by HCE have not been performed yet.

In this article, we investigated the cluster size and the growth mode dependence of the growth rate and the crystallinity of YBCO film deposited by HCE. The possibility of high-quality epitaxial deposition at an extremely high rate by HCE was also surveyed.

II. EXPERIMENT

$YBa_2Cu_3O_{7-x}$ coprecipitated powder consisting of particles 1–2 μm in size was fed into the plasma using a high-performance powder feeder.[4] The powder feed rate (R_{fd}) was determined by monitoring the optical emission intensity of Ba^+ in a plasma flame. Mirror-polished $SrTiO_3$ (100) was used as the substrate. During the growth rate and rocking-

[a]Present address: The Institute of Space and Astronautical Science, 3-1-1, Yoshinodai, Sagamiharashi, Kanagawa 229-8510, Japan; electronic mail: takamura@pub.isas.ac.jp
[b]Electronic mail: norio@plasma.t.u-tokyo.ac.jp

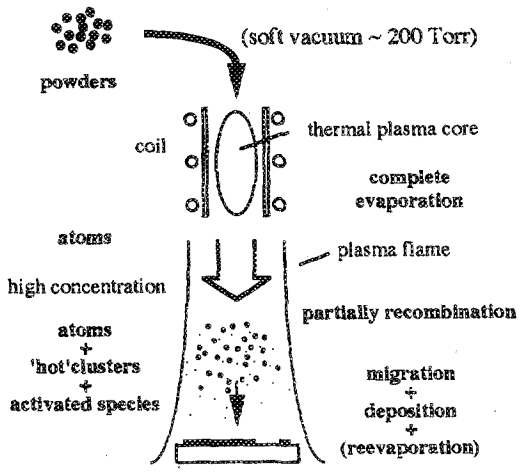

FIG. 1. Schematic of plasma flash evaporation method.

curve measurements (Sec. III A), substrate temperature (T_{sub}) was measured by a thermocouple set inside a substrate holder, as reported previously,[7] to accurately produce the same conditions for comparison. During the high T_{sub} growth experiment (Sec. III B), T_{sub} was measured in terms of the intensity of infrared radiation from the substrate.[9] Cluster size was measured by the microtrench method,[8] and controlled by changing R_{fd} or torch–substrate distance (L).[6,8] Increasing R_{fd} or L resulted in an increase in cluster size. The deposited films were characterized by scanning electron microscopy (SEM), scanning tunneling microscopy (STM), x-ray diffraction (XRD) analysis, and x-ray rocking-curve measurement.

III. RESULTS

A. Feed rate effect on growth rate and epitaxy

To investigate the effects of cluster size and growth mode change on the growth rate (R_g) in HCE, R_g was measured as a function of R_{fd}. Deposition conditions listed in Table I are exactly the same as those in our previous article[7] where 2DCNG was observed at $R_{fd} \geqslant 200$ mg/min. R_g was estimated by SEM observation. Figure 3 shows R_g of YBCO films deposited at a torch–substrate distance L of 310 mm and T_{sub} of 670 °C, along with the growth mode observed by

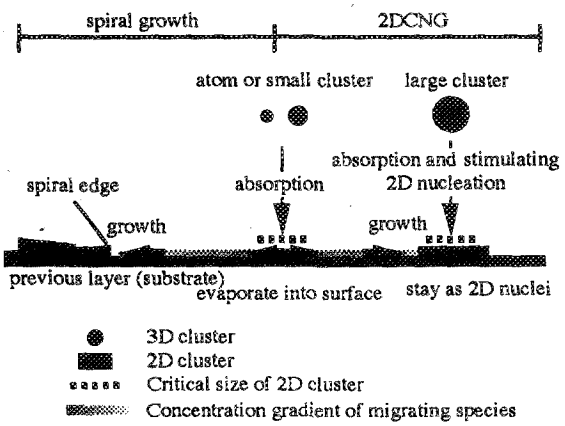

FIG. 2. Schematic description of the behavior of hot clusters on surface.

TABLE I. Typical conditions for YBCO deposition.

Rf power	50 kW
Pressure	200 Torr
O_2 gas	47 SLM
Ar gas	2.4 SLM
Substrate temperature (T_{sub})	670 °C
Torch substrate distance	310 mm
Powder feed rate (R_{fd})	60–500 mg/min
Deposition time	30–120 s

STM and the degree of epitaxy determined by XRD. R_g increases gradually in region A ($0 < R_{fd} < 200$ mg/min), where the growth mode was spiral and well epitaxial films were deposited. R_g is fitted well by the theoretical curve for spiral growth proposed by Burton *et al.*[10] On the other hand, in region B (around $R_{fd} = 200$ mg/min), R_g drastically increased and the growth mode was not spiral but terrace-like and still well epitaxial. Finally, in region C ($R_{fd} > 200$ mg/min), R_g increased constantly and nonepitaxial films with an island-like morphology were obtained. R_g lies on a line passing through the origin, which suggests that in this region, the sticking probability is unity and films grow with an adhesive growth mode.

FWHM of the XRD 2θ–θ scan peak of epitaxial YBCO films deposited by PFE almost agrees with the theoretical limit predicted from film thickness in the spiral and 2DCNG region.[6] Therefore, crystallinity was evaluated from the FWHM of the rocking curve ($FWHM_{rc}$) here. Deposition conditions were the same as those of R_g measurements, except that the thickness of each film was maintained to be 0.6 μm in order to eliminate any effects of thickness on $FWHM_{rc}$. To minimize the broadening of $FWHM_{rc}$ due to 2θ–θ peak broadening from small thickness, a narrow receiving slit of 0.05 mm width was inserted into a 180 mm radius goniometer. Figure 4 shows R_{fd} dependence of $FWHM_{rc}$ of YBCO (005) rocking curve ($2\theta = 38.3°$) at $L = 270$ mm under various T_{sub} conditions. $FWHM_{rc} = 0.065°$ for the single-crystal $SrTiO_3$ (200) rocking curve ($2\theta = 46.0°$), indicating a measurable limit in our system. It is clearly shown that each $FWHM_{rc}$ curve has a minimum with increasing R_{fd}. This means that the crystallinity is improved once with increasing feeding/deposition rate, which seems to be quite unusual for conventional film deposition methods.

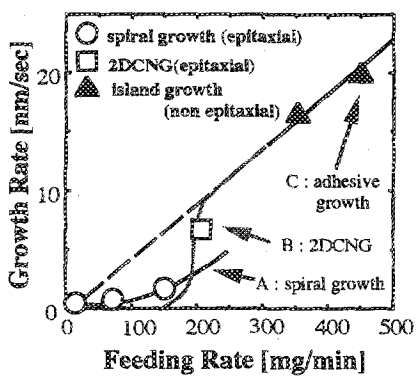

FIG. 3. Feed rate dependence of growth rate, growth mode, and epitaxy. Circles, squares, and triangles indicate the spiral growth, terrace-like growth with no spiral, and island growth, respectively. Open symbols and filled ones indicate epitaxial growth and nonepitaxial growth, respectively.

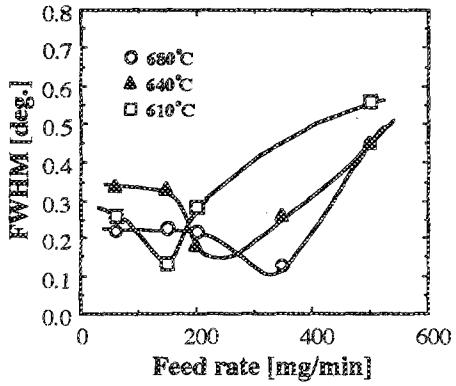

FIG. 4. Feed rate dependence of $FWHM_{rc}$ of YBCO (005) rocking curve.

B. Demonstration of high substrate temperature growth

Figure 5(a) shows the XRD pattern of YBCO film deposited at $T_{sub}=800\,^{\circ}C$, $R_{fd}=300$ mg/min, and torch–substrate distance $L=290$ mm, for 60 s, respectively. $T_{sub}=800\,^{\circ}C$ is slightly higher than our conventional substrate temperature. The average cluster size at the substrate was estimated to be 2 nm under these conditions. The thickness of this film was about 1 μm; therefore, the deposition rate was 16 nm/s, which was $10-10^2$ times faster than those of conventional methods such as sputtering and chemical vapor deposition. The film was strongly c axis and in-plane oriented and no peaks from other phases were observed. Figure 5(b) shows a (005) rocking-curve profile of this film. The $FWHM_{rc}$ was revealed to be less than 0.14°, which is one of the smallest values for YBCO films reported so far.[11,12] Figure 6(a) shows a typical STM image of the same film. The surface of this film was found to be very smooth on the atomic scale with some step structures. The step height was 1.2 nm, which corresponded to the c-axis lattice constant of YBCO. No spirals were found, although it was reported that screw-dislocation-mediated growth such as spiral growth is an intrinsic feature of YBCO thin-film growth.[13] In addition, many disk-shaped terraces of 30–100 nm diameter were observed.

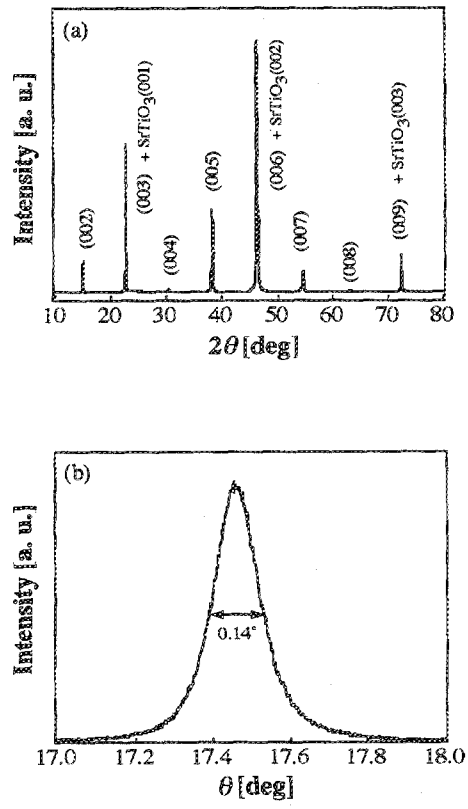

FIG. 5. $2\theta-\theta$ XRD pattern (a) and the (005) rocking curve profile (b) of a $YBa_2Cu_3O_{7-x}$ film deposited from hot clusters.

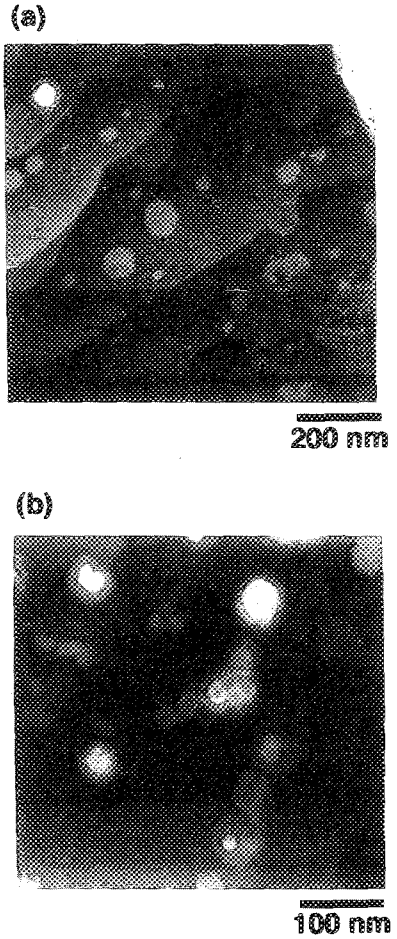

FIG. 6. (a) STM image of 1-μm-thick $YBa_2Cu_3O_{7-x}$ film deposited from hot clusters. (b) STM image of a film deposited from large clusters. Its $FWHM_{rc}$ is 0.18°.

Figure 6(b) shows an STM image of the film deposited at a slightly larger L of 300 mm, which means that the deposition clusters may be larger than those of the film in Fig. 6(a). In this case, the linear steps disappeared and disk-shaped terraces and their combinations were clearly observed. This film had a $FWHM_{rc}$ of 0.18° and was still epitaxial and smooth on the atomic scale, with the exception of steps. The terraces in Figs. 6(a) and 6(b) seemed to originate from the incident hot clusters. These small, disk-shaped terraces were considered to be less stable than large ones because of the Gibbs–Thomson effect and to merge into larger step structures not only during deposition but also during the cooling stage after deposition. Some linear steps such as those observed in Fig. 6(a) were considered to be formed from such disk-shaped terraces.

IV. DISCUSSION

In region B in Fig. 3, the jump in R_g is considered to be caused by 2DCNG. According to the Burton and co-worker's[10] (BCF) and the Kossel[14] crystal growth theory, a crystal grows only at a step or a kink in the lateral direction. For growth in the perpendicular direction, initial growth sites are needed. These next-layer growth sites are supplied by the rotation of steps around screw dislocations (in the BCF case) or by incidental nucleations (in Kossel's case), both of which require a driving force induced by supersaturation. This next-layer generation stage (NLGS) is considered to be the rate-determining process in most cases of the YBCO film growth.[13] In 2DCNG, however, the incoming 3D clusters generated in the plasma flame may enhance 2D nucleation or the clusters themselves may become 2D nuclei,[7] and provide steps or kinks as the next-layer growth sites. This is considered to be the reason why R_g increases even at low supersaturation in region B (Fig. 3). The jump resembles the transition from spiral growth to adhesive growth in Kossel's[14] and BCF[10] theory. In their cases, the transition is caused by an abrupt increase in 2D nucleation rate when the 2D critical nucleus size r_{2D}^* is close to an atom. Simultaneously, the growth changes to adhesive and nonepitaxial. So, based on their theories, it is difficult to explain why the film after a R_g jump remains epitaxial with FWHM 2θ–θ scan of XRD (005) peak of 0.3°.[6] Here, r_{2D}^* seems to be closely related to epitaxial quality. Walton clearly showed that the critical size of a 2D cluster affects the orientation of the next layer; for example, at least four atoms are required for epitaxial growth on square lattice surfaces.[15] Based on this assumption, films grow epitaxially at $r_{2D}^* >$ a critical limit $r_{2D}^{*e} \sim$ few atoms. In Kossel's or Burton *et al.*'s growth theory, both R_g jump and the transition from epitaxial growth to nonepitaxial growth occur under almost the same conditions of r_{2D}^* close to one atom. In the case of 2DCNG, however, R_g jump is caused by incoming clusters at large r_{2D}^*, where $r_{2D}^* \geqslant r_{2D}^{*e}$ and films grow epitaxially. Actually, r_{2D}^* for 2DCNG transition in Fig. 3 was easily estimated from the spiral step width[7] to be about 2.5 nm, which is too large to grow by 2DNG. This model clearly shows why 2DCNG can grow film epitaxially even after R_g increases abruptly. The supersaturation dependence of growth rate for spiral growth, 2DNG, 2DCNG, and adhesive growth is illustrated in Fig. 7. For multicomponent systems, the definition of supersaturation is somewhat ambiguous. Here, similar to our previous article,[7] supersaturation is assumed to be proportional to feed rate (R_{fd}) at a constant temperature. The region B is equal to that of 2DCNG reported previously.[7] In Kossel's growth theory, the supersaturation α for practical growth is so close to that of r_{2D}^{*e} that precise control of α is required for single-crystal growth. In 2DCNG, the α is much lower than that of r_{2D}^{*e} and epitaxial film growth occurs in a wide range of α, which means that no stringent control is required and R_{fd} and T_{sub} can be optimized for film growth under more general conditions. The last advantage is well demonstrated in Sec. III B.

As shown in Fig. 4, crystallinity is improved once with increasing feed rate. This curve can be explained as shown in Fig. 8, where $T_s = 640$ °C. At $R_{fd} < 200$ mg/min, the films exhibited spiral growth and the values of $FWHM_{rc}$ were nearly constant at 0.3°. Interestingly, many YBCO films spirally grown by other conventional processes[16,17] were reported with such $FWHM_{rc}$ closed to 0.3°. This $FWHM_{rc}$ broadening is seemed to be attributed to an intrinsic gradient of planes around screw dislocations. It is well known that the local strain of spiral lattice decreases rapidly with increasing distance (r) from a screw dislocation and is not detectable by XRC. A macroscopic tangential gradient, $\arctan(h/2\pi r)$, however, should be present in a sufficiently relaxed film where h is the length of Burger's vector. For example, in Fig. 9(a), the orientation difference between points a and b, 100 nm apart from the center of a screw dislocation with a 1.2-nm-long Burger's vector, is estimated to be about 0.3°, which should result in $FWHM_{rc} \sim 0.3°$ for spirally grown films with a grain size of about a few hundreds nm, which typically exist on the surface of spirally grown YBCO film. Moreover, in this case, films consist of mosaic crystals around screw dislocations [Fig. 9(b)].

On the other hand, at $R_{fd} > 200$ mg, the films grew by 2DCNG, and in this region, $FWHM_{rc}$ increases monotonically with R_{fd}. The $FWHM_{rc}$ at the beginning of 2DCNG,

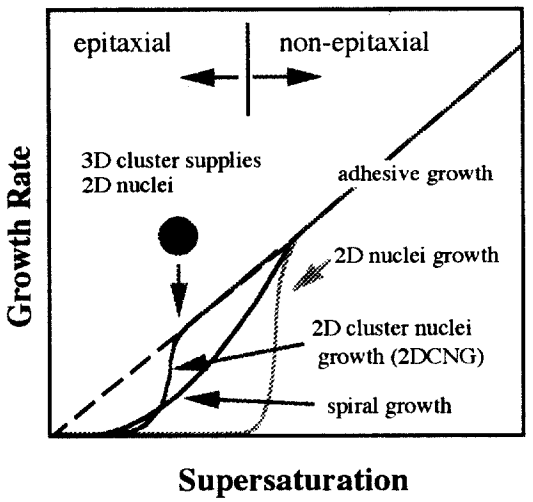

FIG. 7. Schematic of growth rate in various growth modes.

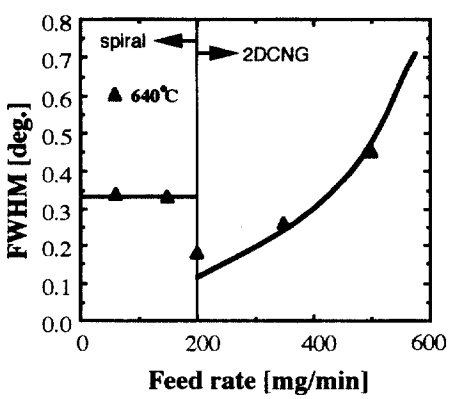

FIG. 8. Feed rate dependence of FWHM of YBCO (005) rocking curve at 640 °C in Fig. 4.

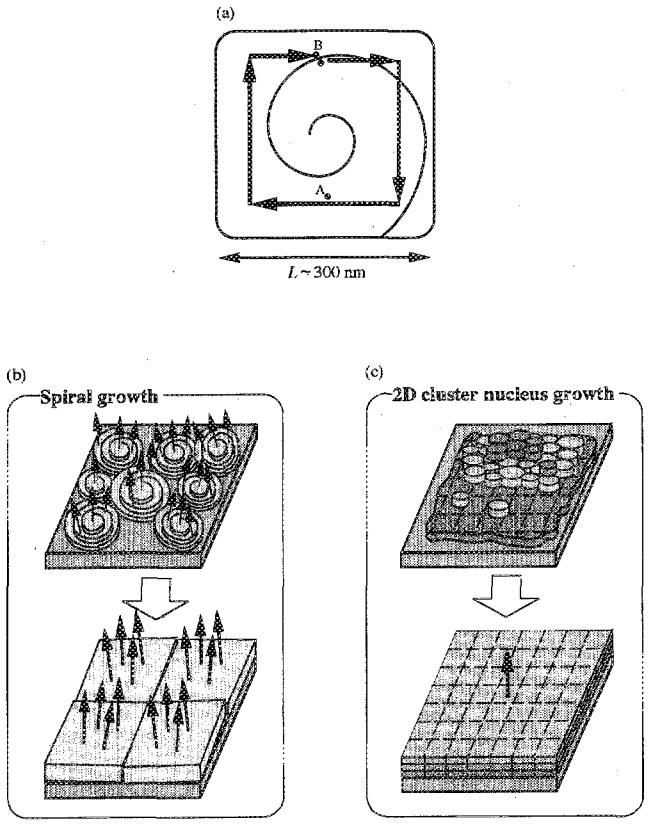

FIG. 9. (a) Estimation of orientation difference perpendicular to the substrate of films with a grain size of 1 μm grown by spiral growth. (b) Schematic of film structure grown by spiral growth. (c) Schematic of film structure grown by 2D cluster nucleus growth (2DCNG).

however, is less than those in the spiral growth region. This may be reasonable, because the morphology of 2DCNG-grown film is similar to that of complete crystal 2DNG grown by Kossel's mechanism [Fig. 9(c)], while spiral-grown films involves defects around screw dislocations as shown in Figs. 9(a) and 9(b). The R_{fd} for minimum $FWHM_{rc}$ increases with increasing substrate temperature. This result agrees with the increase in R_{fd} at the transition point to 2DCNG with increasing temperature.

The deposition with clusters results in larger sticking probabilities than that with atoms even under low supersaturation conditions, as mentioned above. This may contribute much to the film growth particularly at high substrate temperatures rather than low R_{fd}; both high quality and high growth rate may be achieved simultaneously. In general, high substrate temperature enhances lateral diffusion and atomic rearrangement required to attain high-rate deposition of good films. However, it also reduces the rate of NLGS markedly, resulting in no growth during conventional deposition from atoms. For 2DCNG, however, rate of NLGS is expected to be high owing to high density of growth sites directly formed by the incoming clusters even at high substrate temperatures. This feature explains well why such high-quality films were obtained at an extremely high growth rate at high substrate temperatures using this method in Sec. III B.

HCE may be comparable to liquid-phase epitaxy from the viewpoint of high growth rate for equilibrium phases near the melting points. This method still inherits some advantages of vapor phase deposition, especially the epitaxial growth of phases that do not bound on liquid phase directly or closely in their phase diagram, such as the peritectic phase frequently found in multicomponent systems.

V. CONCLUSION

This study demonstrated the advantages of hot cluster epitaxy for high-rate deposition of epitaxial films. The deposition rate of YBCO films by hot cluster epitaxy increased markedly with the growth mode change from spiral to 2DCNG, and after this transition, films remained epitaxial. Near this transition, films had a minimum FWHM of the rocking curve, which meant maximum crystallinity. Even at high substrate temperatures, this method was able to deposit YBCO film at a practically high growth rate by 2DCNG, resulting in an excellent film with an extremely high growth rate. A 1-μm-thick YBCO film with FHWM of the rocking curve $<0.14°$ and a monolayer-order smooth surface was successfully deposited from clusters of about 2 nm size at a rate of 16 nm/s. These features are well explained if incoming 3D clusters stimulate 2D nucleation on the high-temperature growth surface, high enough to rearrange clusters, but too high for atoms to attain the 2D nucleation, which is a strong rate-determining process in this case.

ACKNOWLEDGMENT

This work was supported by the Japan Society for the Promotion of Science under the program "Research for the Future: JSPS-RFTF97R15301."

[1] *Thermal Plasma Applications in Materials and Metallurgical Processing*, edited by N. ElKaddah (The Minerals, Metals & Materials Society, Warrendale, Pennsylvania, 1992).
[2] K. Terashima, K. Eguchi, T. Yoshida, and K. Akashi, Appl. Phys. Lett. **52**, 1274 (1988).
[3] K. Terashima, T. Akagi, H. Komaki, and T. Yoshida, J. Appl. Phys. **71**, 3427 (1992).
[4] Y. Hirokawa, Y. Takamura, H. Komaki, K. Terashima, and T. Yoshida, J. Mater. Synth. Process. **1**, 53 (1993).
[5] S. Yuhya, K. Kikuchi, Y. Shiohara, K. Terashima, and T. Yoshida, J. Mater. Res. **7**, 2673 (1992).
[6] Y. Takamura, K. Hayasaki, K. Terashima, and T. Yoshida, Plasma Chem. Plasma Process. **16**, 141S (1996).
[7] K. Hayasaki, Y. Takamura, N. Yamaguchi, K. Terashima, and T. Yoshida, J. Appl. Phys. **81**, 1222 (1997).
[8] Y. Takamura, K. Hayasaki, K. Terashima, and T. Yoshida, J. Vac. Sci. Technol. B **15**, 558 (1997).
[9] T. Hattori, N. Yamaguchi, K. Terashima, and T. Yoshida, *Proceedings of the 13th International Symposium on Plasma Chemistry Beijing*, 1997, *Vol. III*, p. 1065.
[10] W. K. Burton, N. Cabrera, and F. C. Frank, Philos. Trans. R. Soc. London, Ser. A **243**, 299 (1950).
[11] M. Schieber and Y. Ariel, Appl. Phys. Lett. **61**, 970 (1992).
[12] C. S. Chern *et al.*, Appl. Phys. Lett. **58**, 185 (1991).
[13] D. G. Schlom, D. Anselmetti, J. G. Bednorz, Ch. Gerber, and J. Mannhart, J. Cryst. Growth **137**, 259 (1994).
[14] W. Kossel, Naturwissenschaften **18**, 901 (1930).
[15] D. Walton, J. Chem. Phys. **37**, 2182 (1962).
[16] S. Williams *et al.*, J. Appl. Phys. **72**, 4798 (1992).
[17] R. Kromann *et al.*, J. Appl. Phys. **71**, 3419 (1992).